Chinese Journal of Polar Science, Vol. 19, No. 2, 193 - 211, December 2008

Modeling the ocean circulation in the Bering Sea

Hu Haoguo[1] and Wang Jia[2]

1 Cooperative Institute for Limnology and Ecosystems Research (CILER), School of Natural Resources and Environment (SNRE), University of Michigan., 4840 S State Road, Ann Arbor, Michigan 48108, USA

2 NOAA Great Lakes Environmental Research Laboratory (GLERL), 4840 S State Road, Ann Arbor, Michigan 48108, USA

Received September 20, 2008

Abstract With parameterized wave mixing, the circulation and the tidal current in the Bering Sea were simulated simultaneously using the three-dimensional Princeton Ocean Model. The simulated circulation pattern in the deep basin is relatively stable, cyclonic, and has little seasonal change. The Bering Slope Current between 200-1000 m isobaths was estimated to be 5 Sv in volume transport. The Kamchatka Current was estimated to be 20 Sv off the Kamchatka Peninsula. The Bering shelf circulations vary with season, driven mainly by wind. These features are consistent with historical estimates. A counter current was captured flowing southeastward approximately along the 200 m isobath of the Bering Slope, opposite to the northwestward Bering Slope Current, which needs to be validated by observations. An upwelling current is located in the shelf break (120-1000 m) area, which may imply the vertical advection of nutrients for supporting the Bering Sea Green Belt seasonal plankton blooms in the break-slope area. The Bering Slope Current is located in a downwelling area.

Key words Arctic Ocean, the Bering Sea, ocean circulation.

1 Introduction

The Bering Sea is a semi-enclosed subpolar sea, which is connected to the Arctic Ocean on the north, and bounded on the west by Russia, on the east by Alaska, and on the south by the Aleutian Islands (Figure 1, model domain). Bowers Ridge (with a minimum depth of 184 m) and Shirshov Ridge (with minimum depth of 500 m) divide the Bering Sea into three basins—the Bowers Basin, the Kamchatka Basin, and the Aleutian Basin. The Bering Sea is divided almost equally between deep basins and the continental shelves (< 200 m). The broad shelf in the east contrasts with the narrow shelf in the west. The steep bathymetric features include the deep Aleutian Trench (> 5500 m) and the Bering Basin (> 3500 m) and the relatively shallow Aleutian (< 100 m) Islands chain, which challenges all the 3-D physical ocean models with sigma coordinates[1].

Observations show the circulation pattern (Figure 2, after *Stabeno et al.*, 1999[2]) in the deep Bering Sea basin is often described as a cyclonic gyre[2]: the Aleutian North Slope Current (ANSC) flows eastward along the Aleutian Islands; the Bering Sea Slope Current

flows northwestwardly, and the southward flowing Kamchatka Current forms the western boundary current. Observations [3] show the currents on the Bering Sea shelf are basically northward or northwestward. However, measurements are not sufficient to determine the seasonal circulation variation, and it also cannot represent the whole domain with sufficient spatial coverage. Models with realistic settings can help to derive more detailed information about the general circulation in the Bering Sea. Overland *et al.* (1994) [4] used a three-layer hydrodynamic model to simulate the circulation of the Bering Sea Basin, while the Bering Sea shelf and slope regions shallower than 500 m, hence the cross-shelf flux, were excluded from the model. Several other models were applied to parts of the Bering Sea [5,6]. Thus, the general circulation pattern is still not well understood.

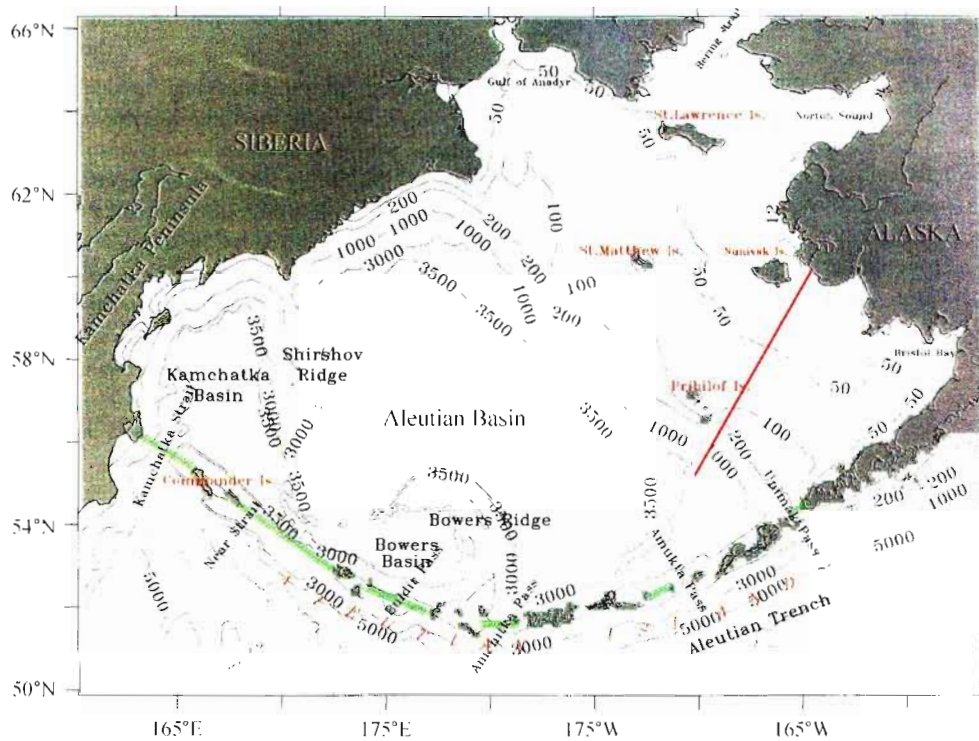

Fig. 1 Model domain and bathymetry of the Bering Sea (in meters). The depths along Aleutian Islands and passes were modified according to NOAA ocean charts. Red line indicates the transect in the text.

Observations show that the cold water ($<1.0°C$) near the bottom in the middle shelf persists throughout the summer [7]. It was speculated that this cold water is formed locally in winter and insulated by strong stratification in summer. The mechanism of thermocline formation seems well understood, i. e., by tidal stirring and surface wind-wave mixing; whereas, it is still difficult to reproduce circulation, themocline, and fronts using a 3-D baroclinic physical ocean model. Overland *et al.* (1999) [8] used a one-dimensional model to hindcast the 1980 spring-summer thermal transition of the Bering Sea shelf as a function of water depth, but without horizontal processes.

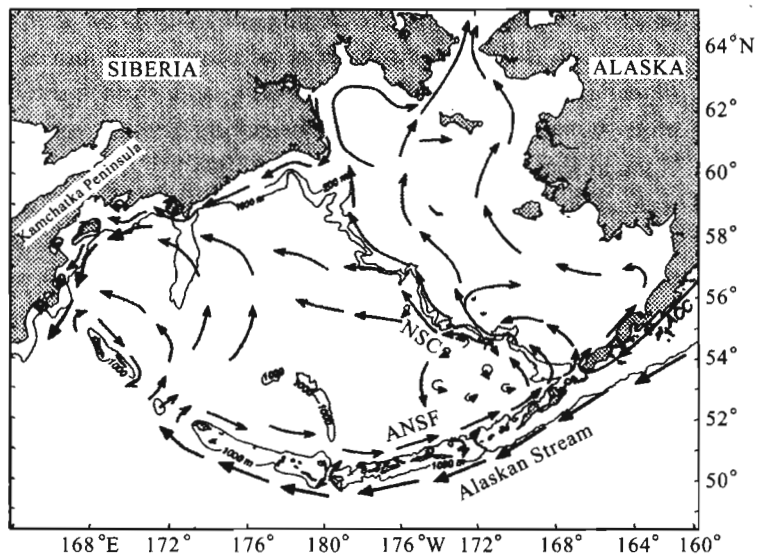

Fig. 2 Schematic diagram for surface circulation pattern in the Bering Sea based on historical observations (reproduced from *Stabeno et al.* 1999).

Thus, a systematic modeling approach in a basin scale that covers both the deep basins and shelves appears to be essential to simulate the circulation and tidal current simultaneously. Since few basin-wide 3-D ocean models exist for modeling ocean circulation and tidal current, we attempt to develop such a model with parameterizations of wind-wave mixing for the study of 1) the circulation and transports of major current systems and 2) dynamic features in the shelf-slope region such as the Bering Slope Current. This paper is organized as follows: Section 2 describes the model configuration; Section 3 discusses simulated results in comparison with available observations, followed by conclusions and discussion in Section 4.

2 The model description

The model used here is the Princeton Ocean Model (POM) described in detail by Blumberg and Mellor (1987)[9] and Mellor (2004)[10]. It is a three-dimensional, primitive-equation, vertical σ-coordinate model and horizontal grid using curvilinear orthogonal and an Arakawa C-grid. Horizontal time differencing is explicit, whereas the vertical differencing is implicit; the latter eliminates time constraints for the vertical coordinate and permits the use of fine vertical resolution in the surface and bottom boundary layers. Complete thermodynamics is implemented. POM has a free surface with a second-order turbulence closure scheme[11] to calculate vertical mixing coefficients. Horizontal mixing coefficients employ the Smagorinsky parameterization.

2.1 Wave mixing parameterization

The modeled surface boundary layer is often too shallow in temperature and salnity dur-

ing the spring-summertime warming[12] and freshening even using the 2.5 closure turbulence model. One major reason is that the mechanic wind-wave mixing processes are not included. *Craig and Banner* (1994)[13] used wave breaking as a surface diffusion boundary condition, which is proportional to u_τ^3, where u_τ is the surface friction velocity. *Mellor and Blumberg* (2004)[10] found that the *Craig and Banner* (1994)[13] model does deepen the mixed layer in a 1-D calculation, and has a positive, but relatively small influence on the 3-D calculation. *Ezer and Mellor* (1997)[14] proved that the absorption of short wave radiation below the surface, due to the loss of surface heat, causes the upper layer to be less stable, increases mixing, and thus deepens the summertime thermocline. In this paper, surface wave mixing is parameterized into the model as in Hu *et al.* (2004)[15]:

$$K_{wm} = \frac{2k^2}{g}\delta\beta^3 U^3 e^{\frac{gz}{\beta^2 U^2}}$$

K_{wm} is the wave mixing coefficient, β is the wave age, δ is the wave steepness, U is the wind speed, z is depth, and $k=0.4$ is the *Karman* constant. A mature wave is assumed in this study, then set $\beta=1.0$, $\delta=0.1$.

Heat diffusion coefficient K_{hm} can be assumed equal to K_{wm}. Since in general, heat mixing is considered to be slower than momentum transfer, $K_{wh}=PW_{wm}$ is assumed, where P is an empirical constant depending on the Richardson number. Following the POM[16], we set

$$K_{hm} = \frac{S_H}{S_M}K_{wm}$$

where

$$K_m = qlS_M, \quad K_h = qlS_H$$
$$S_H[1-(3A_2B_2+18A_1A_2)G_H] = A_2(1-6A_1/B_1)$$
$$S_M(1-9A_1A_2G_H) - S_H[(18A_1^2+9A_1A_2)G_H] = A_1(1-3C_1-6A_1/B_1)$$
$$(A_1, B_1, A_2, B_2, C_1) = (0.92, 16.6, 0.74, 10.1, 0.08)$$
$$G_H = \frac{l^2}{q^2}\frac{g}{\rho_0}\left(\frac{\partial\rho}{\partial z} - \frac{1}{c_s^2}\frac{\partial p}{\partial z}\right)$$

where K_m is the vertical turbulence momentum viscosity coefficient, K_h is the vertical turbulence heat diffusion coefficient, q is the turbulence velocity, l is the turbulence mixing length scale, c_s is the sound velocity, ρ is the water density, ρ_0 is the reference density, P is the pressure, and G_H is the Richardson number.

If K_{wm} and K_{wh} are the vertical viscosity and diffusion coefficient calculated by the level 2.5 closure turbulence model, the total mixing coefficients are

$$K_h' = K_h + K_{wh}; \quad K_m' = K_m + K_{wm}$$

2.2 *Tidal mixing*

Tides provide the most important and periodic driving force in the Bering Sea. The tides and tidal currents on the Bering Sea shelf play an important role in such oceanographic processes as the maintenance of the density structure, sediment resuspension and nutrients transport. Circulation can be simulated without tide and it is acceptable when the tidal current is weak in the deep ocean/sea. However, since the tidal current is very strong in the

Bering Sea shelf compared to the circulation, the tidal energy accounts for 90% of the total energy[3], dominating tidal stirring should not be ignored. Thus, the tidal current is in this study.

The open boundary conditions of velocities were given by

$$V_{total} = V_{circulation} + \sum_{i=1}^{n} (V_a)_i \cos(\omega_i t + \theta_i)$$

where V_a is tidal amplitude, θ is tidal phase, ω is the tidal frequency, and n is the number of tidal constituents.

2.3 *Model configuration*

The horizontal grids have a spherical coordinate system with a resolution of 1/12° longitude (about 9.3 km) and 1/6° latitude (from 10 km near the Aleutian Islands to 7.4 km in the Bering Strait.) There are 24 σ layers in the vertical, $\sigma = (z - \eta)/(H + \eta)$, where $\eta(x, y)$ and $H(x, y)$ are the surface elevation and water depth, respectively. The vertical resolution is higher near the surface and the bottom for a better representation of the surface and bottom boundary layers. Vertical levels were defined at $\sigma = 0$, -0.008, -0.016, -0.031, -0.063, -0.125, -0.188, -0.250, -0.313, -0.375, -0.438, -0.500, -0.563, -0.625, -0.688, -0.750, -0.813, -0.875, -0.938, -0.969, -0.984, -0.992, -0.996, -1. The model has split modes. The 2-D external mode uses a time step of 20 seconds, and the 3-D internal mode uses time step of 600 seconds.

Bathymetry is obtained from 5-minute resolution ETOPO05 data; however the depths of the Aleutian Islands and passes were modified according to NOAA ocean charts (NOAA Chart). Smoothing of topography was conducted for the steep slopes. Subtracting the area-averaged climatological density field before calculating pressure gradient terms was applied to substantially reduce errors to be less than 10% of the mean flow and other numerical errors[16][14]. The above procedure is widely used in previous applications of σ coordinate models. The maximum bottom slope allowed between two adjacent grid points is $\Delta H/H < 0.1$. Maximum and minimum depths were set to 3000 m and 10 m, respectively. Upwind advection boundary conditions allow the advection of the monthly mean temperature and salinity into the model domain under inflow conditions. At the open boundaries, vertically-averaged inflow/outflow was prescribed on the basis of observations (described later). For the baroclinic velocities, Sommerfeld type radiation conditions were used[17]. Observations since the 1940s show that the annual mean net northward transport is about 0.8 Sv in the Bering Strait[18-22], and seasonal variations exist with a larger transport in summer than in winter. Therefore, the outflow transport was specified according to the monthly data.

Volume transport of the Alaskan Stream has been described by direct and indirect measurement data. *Cokelet et al.* (1996)[23] used vessel-mounted Acoustic Doppler Current Profiler (ADCP) measurements to obtain an Alaskan Stream transport of 24 Sv based on an absolute reference for geostrophic currents (0/1500 db). Onishi and Ohtani (1999)[24], using current-meter mooring data, show that the Alaskan Stream volume transport (referred to 3000 m) is 27.5 ± 6.5 Sv. Reed and Stabeno (1999b)[25] used CTD (Conductivity/Temperature/Depth) casted data to obtain a volume transport of 25 Sv

(referred to the bottom). The westward flowing Alaskan Stream was specified at the western open boundary with a constant throughput of 25 Sv. The eastern boundary inflow is 29 Sv plus a transport that equals the northward outflow at the Bering Strait.

The model was initialized with the annual climatological temperature and salinity data from the Polar science center Hydrographic Climatology (PHC 3. 0, Steele *et al.* 2001[26]). The sea ice model in the Bering Sea was not included in this study. Monthly sea surface temperature (SST) and salinity (SSS) data were used as the surface boundary conditions. Because our in this study focus is only on seasonal variation of ocean circulation in this study, monthly mean wind stress data was used from the Comprehensive Ocean-Atmosphere Data Set (COADS). The monthly mean data were interpolated linearly to each time step.

Then, we re-ran the model for another four years using the previous sixth-year output as the restart or initial conditions. During the four-year run, all the monthly atmospheric forcings remained the same. Then, the last year variables were used for examining the seasonal cycle in this study.

3 Simulation results

3. 1 The validation of tides and tidal residual current

Two harmonic analyzed co-amplitude (solid lines) and co-phase (dashed lines) maps of the principal semidiurnal lunar constituent M_2 and diurnal lunar constituent K_1 are shown in Fig 3. A small change in amplitude and phase occurs in the deep basin. The amplitude increases slowly from the deep basin to the shallow shelf, while it increases dramatically close to the Alaskan coast, especially in Bristol Bay, and the maximum amplitude exceeds

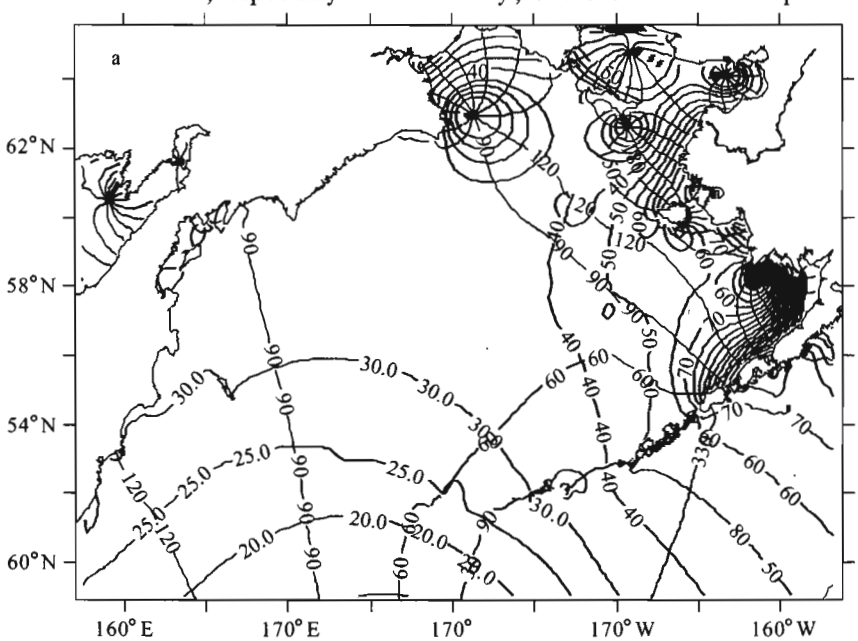

(referred to the bottom). The westward flowing Alaskan Stream was specified at the western open boundary with a constant throughput of 25 Sv. The eastern boundary inflow is 29 Sv plus a transport that equals the northward outflow at the Bering Strait.

The model was initialized with the annual climatological temperature and salinity data from the Polar science center Hydrographic Climatology (PHC 3. 0, Steele *et al.* 2001[26]). The sea ice model in the Bering Sea was not included in this study. Monthly sea surface temperature (SST) and salinity (SSS) data were used as the surface boundary conditions. Because our in this study focus is only on seasonal variation of ocean circulation in this study, monthly mean wind stress data was used from the Comprehensive Ocean-Atmosphere Data Set (COADS). The monthly mean data were interpolated linearly to each time step.

Then, we re-ran the model for another four years using the previous sixth-year output as the restart or initial conditions. During the four-year run, all the monthly atmospheric forcings remained the same. Then, the last year variables were used for examining the seasonal cycle in this study.

3 Simulation results

3. 1 The validation of tides and tidal residual current

Two harmonic analyzed co-amplitude (solid lines) and co-phase (dashed lines) maps of the principal semidiurnal lunar constituent M_2 and diurnal lunar constituent K_1 are shown in Fig 3. A small change in amplitude and phase occurs in the deep basin. The amplitude increases slowly from the deep basin to the shallow shelf, while it increases dramatically close to the Alaskan coast, especially in Bristol Bay, and the maximum amplitude exceeds

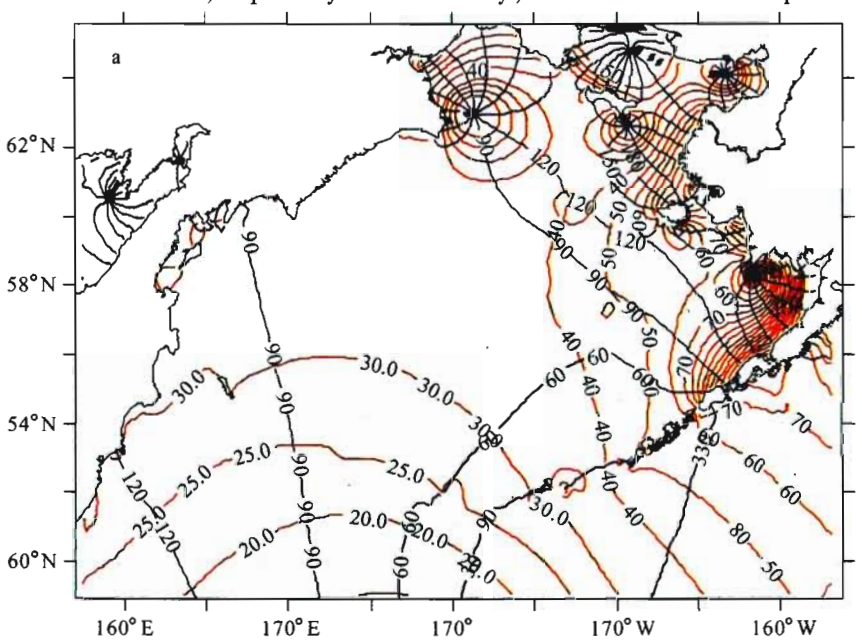

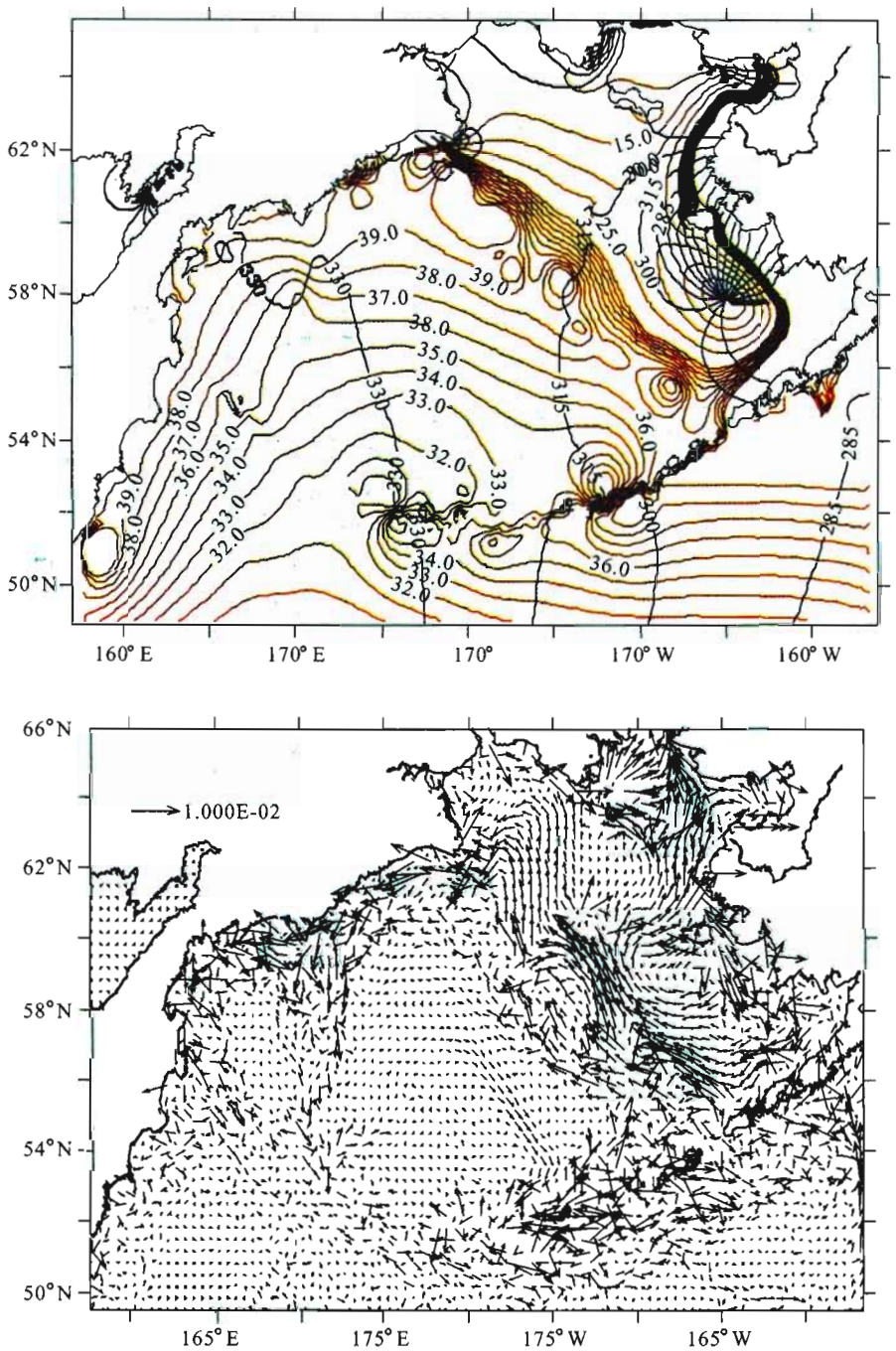

Fig. 3 a) computed amplitude (solid line, in centimeters) and phase (dashed line, in degrees) of the semidiurnal M_2; b) computed amplitude (solid line, in centimeters) and phase (dashed line, in degrees) of the semidiurnal K_1, c) computed residual tidal current (m/s).

2 meters. There are five M2 amphidromic points due to tidal waves interference/superposition: in the western Gulf of Anadyr, in the northern Norton Sound, in Bristol Bay, in the

south of St. Lawrence Is., and at (167°W, 54°N). These results are similar to the previous studies[27].

Differing from the M_2 distribution, the K_1 amplitude increases from the open ocean, deep basin to the Bering Slope and then decreases in the outer-middle shelf, but again quickly increases near the Alaskan coast. A notable feature is that the K_1-amplitude reduces sharply across the Bering Slope, which was also observed by Kowalik (1999)[27] such that a tidal waves propagating into the continental slope and shelf areas locally induce topographic waves where the local period of rotational-gravitational mode is equal to the tidal period. Tidally-generated topographic waves occur only in the regions poleward from the critical latitude: the latitude is 30N for K_1 tide and 74.5N for M_2. Thus, only diurnal topographic waves can be generated.

The energy of the basic tidal constituents is transferred toward longer periods and the tidal currents averaged over tidal period generate residual current. The tidal stirring significantly affects local vertical mixing and accelerates the resuspension of sediments and the release of nutrients. The residual tidal current contributes to long-term transport of nutrients and particle materials. Measurement of residual tidal currents is almost impossible because it is difficult to separate the tidal residual currents from wind-generated current (also residual). In this study, a tide only model was implemented to examine the tidal residual current.

The tidal residual current (also called Lagrangian residual current) was calculated by

$$U_R = \frac{1}{T}\int_0^T u dt + \frac{1}{TD}\int_0^T u\eta dt$$

where T is the tidal period, u is the tidal velocity, D is the water depth, and η is the sea surface elevation. The first term on the right side is called the Eulerian residual current and the second term is called the Stocks' residual current. The result is shown in Figure 3c, plotting every 4-grids in both longitude and latitude. The tidal residual currents in the middle shelf and outer shelf flow consistently northwestward or northward with a magnitude of about 0.5 cm/s, and part of the residual currents flows into Bering Strait. This may indicate the long-term transport of material and neutrient transport from the southern Bering Shelf to the northern Bering Shelf, and to the Arctic Ocean via Bering Strait.

3.2 General Circulation and Transport

The simulated summer circulations (Figure 4a) show that the Alaskan Stream flows westward along the Aleutian Islands and enters the Bering Sea via the Aleutian Passes mainly from the Kamchatka Strait, the Near Strait, the Amchitka Pass, the Amukta Pass, and the Unimak Pass. Water enters the Bering Sea from the eastern side of the Kamchatka Strait and the Near Strait and flows eastward along the north side of the Commander Islands towards the Bowers Ridge. This current is not well documented except for a schematic diagram of the Bering Sea circulation pattern (Figure 2). This current flows clockwise along the isobaths of the Bowers Ridge; part of the flow turns eastward at 178°E, 56°N and enters the Aleutian Basin gyre, and the other part turns westward to form the clockwise Bowers Basin gyre.

The water from Bowers Ridge flows eastward from Amichikta Island to Unimak Island,

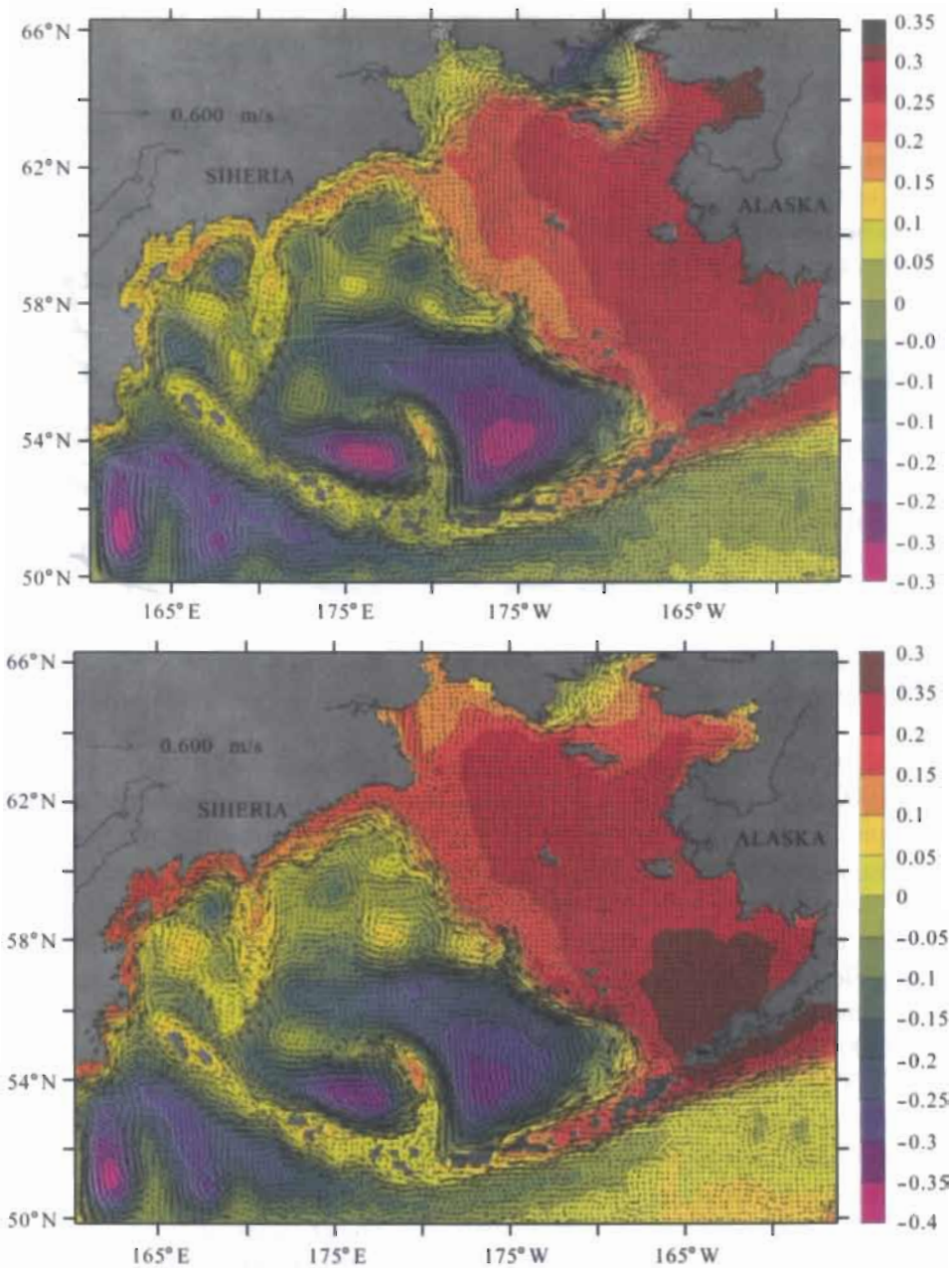

Fig. 4 The modeled Bering Sea surface circulation in July (upper panel) and February (lower panel). Color bar indicates sea surface elevation (in meters).

which is well documented and named as ANSC[27]. The transport of the ANSC was estimated to be about 2-4 Sv based on satellite-tracked drifting buoys and geostrophic flow referred to 500 db[28]. The modeled transport of the ANSC is 5 Sv if the integration is conducted from the Islands to the 2000 m isobath (Figure 5), and increase to 10 Sv if the integration is conducted from the islands to the 3000 m isobath.

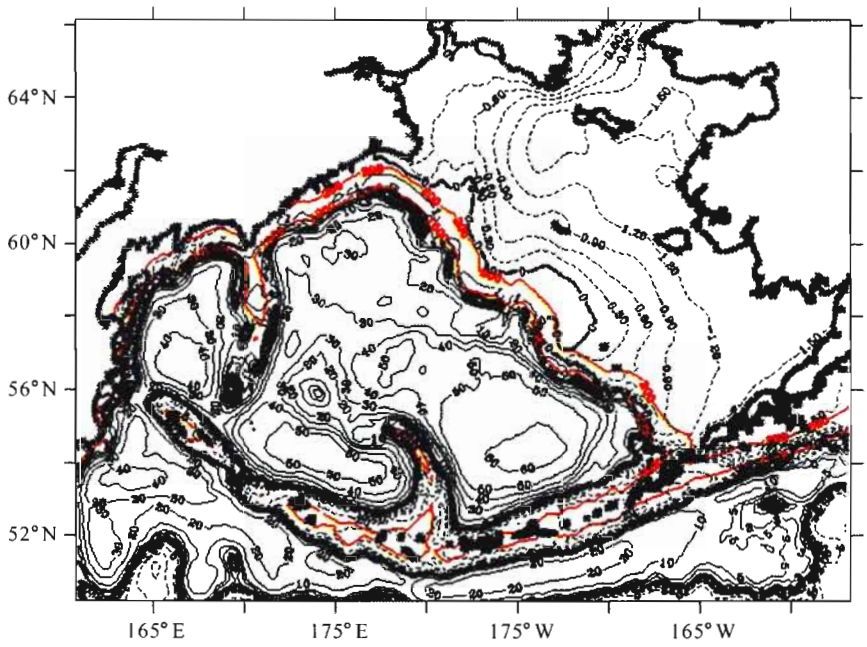

Fig. 5 Model-simulated stream function or transport in July (in Sverdrup, 1 Sv = 10^6 $m^3 s^{-1}$). The red contours indicate 200 m and 1000 m isobaths.

The ANSC turns northwestward at the Bering Slope (about 167°W, 55°N), then flows along the 1000-3000 m isobaths on the Bering Slope to form the Bering Slope Current. The Bering Slope Current becomes wider at 175°W, 56°N and bifurcates into two branches: one branch flows westward into the Aleutian Basin and contributes to the northwest Aleutian Basin gyres; the other branch flows along the 1000-3000 m isobaths to the slope of Kamchatka. Between the two branches there are large eddies, both clockwise and anticlockwise. The Bering Slope Current keeps flowing southwestwardly parallel to the Siberian coast. The transport in the Bering Slope Current is about 5 Sv (Figures 5), which is integrated from 200 m to 1000 m isobaths. Note that the transport increases to 10 Sv if the integration is extended to 2000 m. The bathymetric feature of the Shirshov Ridge causes a southward deflection and reduction in speed. Some part of the water flows southward along the east side of the Shirshov Ridge, and then merges into the ANSC. The other part of the water crosses the Ridge and enters the Kamchatka Basin.

In the Kamchatka Basin there are several large eddies (Figures 4a). An anticlockwise eddy has a diameter of about 360 km with the center at 168°E, 59°N. The other clockwise eddy has a diameter of about 400 km with the center located at about (167°E, 57°N). There are mesoscale eddies on the right side of the two large eddies. The Alaska Stream enters the Kamchatka Basin from the eastern Kamchatka Strait and flows northward until 58°N, then turns west to merge with the Kamchatka Current, which flows southward and leaves the Kamchatka Basin from the western Kamchatka Strait. The transport of the Kamchatka Current integrated from coast to 3000 m isobath is about 20 Sv (see Figure 5), consistent with the data-assimilated model estimate of 14-24 Sv by Panteleev *et al.* (2006)[29].

A current with an order of 1.0 Sv along the east coast of Siberia (173°E, 61°N),

which originates from part of the Bering Slope Current water, turns northward at (173°E, 61°N), flows northeastward clinging to the coast, passes around Cape Navarin, and enters the Gulf of Anadyr. The clockwise current exits the Gulf from Anadyr Strait west of St. Lawrence Island and flows to the Bering Strait (Figure 4a). However, this current is weak in winter (Figure 4b). Data from observed temperature, salinity, buoy drifters[29], and the summer nitrate concentration in the Anadyr Water all confirm that the current enters the Gulf of Anadyr from the south of Cape Navarin, parallel to the Siberian coast on the Gulf of Anadyr, turns eastward, flows to the Strait of Anadyr, and then flows into the Bering Strait[30].

The winter circulation pattern (Figure 4b) is similar to that in summer, except that 1) the current in the Gulf of Anadyr is weaker (5 cm/s) than in summer (10 cm/s), and 2) the shelf current is stronger in winter than in summer.

The stream function (Figure 5) and major current transports were calculated based on our model simulation. Overall, the general circulation in the deep basin is cyclonic. The overall transport in the Aleutian Basin, the Kamchatka Basin, and the Bowers Basin are estimated in the upper 3000 m to be 60 Sv, 40 Sv, and 50 Sv, respectively. The barotropic circulation in the Bering shelf is about 1.2 Sv, while the wind driven circulation contributes about 0.3 Sv, totaling an 1.5 Sv transport on the Bering shelf (see Figure 5). Although the inflow condition for the Alaskan Stream is 29 Sv, the Alaskan Stream can have a transport up to 30 Sv, while the circulation downstream of the Alaskan Stream (see the left corner of Figure 5) can reach about 40 Sv.

Topography is a well-known important dynamic factor for veering the ocean circulation in the Bering Sea . Figure 6 shows a clear picture of the 1 0 0 - m circulation pattern that

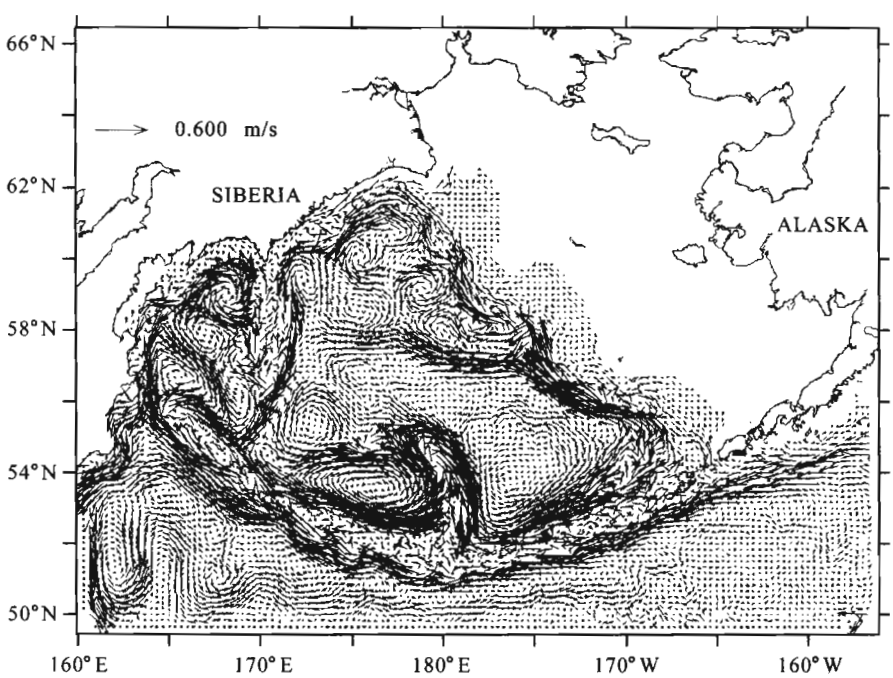

Fig. 6 Model-simulated ocean current field at 100 m depth.

veered by topography. For instance, the Bering Slope current is veered by the Bering Slope until it reaches a ridge at (176W, 57.5N), causing a bifurcation into two branches. The Shirshov and Bowers Ridges clearly veer the current that flows along the isobaths. The Kamchatka Current is another example that bears the signature of both the topography and coastline.

3.3 The Bering Sea shelf circulation

The summer vertically-averaged circulation on the Bering Sea shelf (Figure 7a) is relatively weak (<5 cm/s), flowing northwestward or northward. The water enters from the Unimak Pass bifurcated into two branches: one branch flows directly into the Bering Slope along the 200-m isobath via the east side of the Pribilof Islands, then flows (3-4 cm/s) northwestward along about 100-m isobath, and eventually joins the current of the Gulf of Anadyr in the Bering Strait. Most of the Anadyr Current flows along the Siberian coast, which agrees with the observations[18,30]. The other branch (about 3-4 cm/s) flows northeastward along the Alaska Peninsula into Bristol Bay. The current in Bristol Bay flows anticlockwise along the isobaths, and bifurcates as it exits the bay. One branch (about 2-3 cm/s) flows approximately along the 50-m isobath northwestward in the middle shelf and enters the Bering Strait. The other branch (1-2 cm/s) flows northward along the Alaska coast, passes the Nunivak Strait, turns anticlockwise (5 cm/s) in the mouth of the Norton Sound, and enters the Bering Strait.

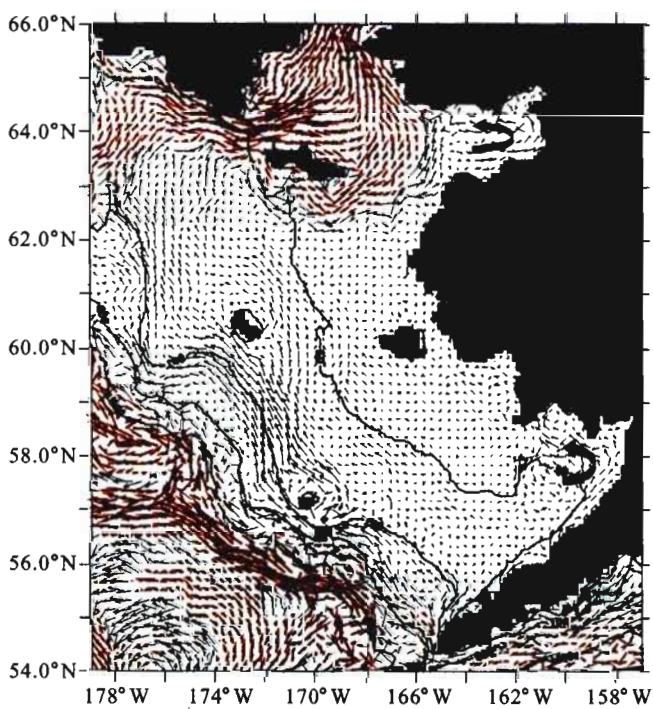

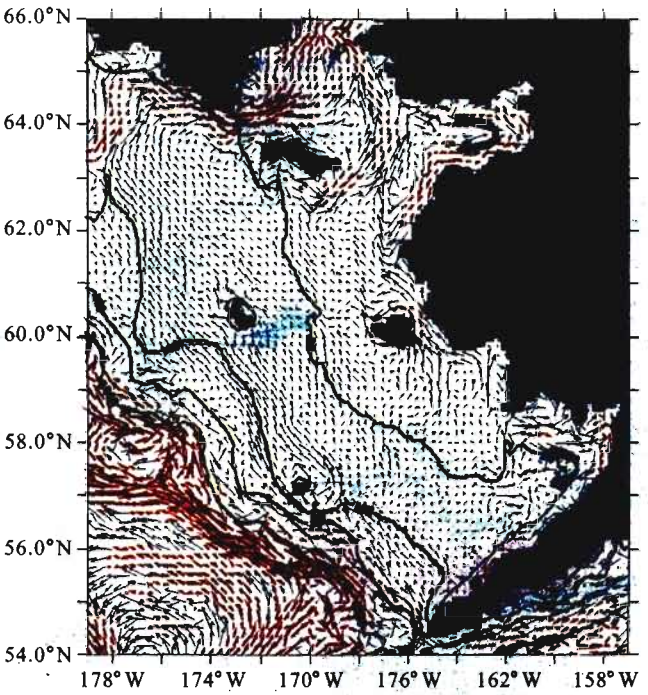

Fig. 7 Model-simualted Bering Sea Shelf vertically-averaged current in summer (upper panel) and in winter (lower). Black arrows indicate current velocity smaller than 10 cm/s and red arrows indicate current velocity greater than 10 cm/s. The green contours denote isobaths in meters. The thickened arrows show cyclonic/anticyclonic (anticlockwise/clockwise) circulation patterns in Bristol Bay and Norton Sound in summer/winter.

The winter circulation is similar to the summer circulation in the middle and outer Bering Shelf (Figure 7b), but with a larger magnitude due to predominant wind forcing. The surface current direction differs from the bottom current direction. The surface current follows the wind direction, whereas the vertically-averaged current flows northerly or northwestwardly. In the inner shelf, the currents vary noticeably. The water exiting from Bristol Bay flows southwestward to 163°W, 55°N along the north of the Alaska Peninsula. This current in Nunivak Strait becomes strong (about 5 cm/s) and flows northward. The currents in Bristol Bay and in Norton Sound flow clockwise in winter compared to the anticlockwise circulation in summer, consistent with previous observations[3].

3.4 The shelf-break counter current?

Just north of the Bering Slope Current, the model captures a narrow (30-50 km) counter current (Figure 8) almost parallel to the Bering Slope Current, which extends from 179°E, 62°N to 168°W, 55°N along about 200 m isobath. The current tends to be stronger while it flows southeastward possibly because of the entrainment of water from both the shelf and the Bering Slope Current. The entrained water from the shelf is mainly located at 176 – 178°W, 59°N, while the entrained water from the basin is located at about 173 – 172°W, 57°N. This counter current is stronger in summer (from July to November, about 5-6 cm/

s) than in winter-spring (from December to June, about 3-4 cm/s). The model results show that the Bering Slope Current provides major water to the counter current. Although a current vector opposite to the Bering Slope Current was observed near the 200-m isobath (see S11 in Fig. 2 of Cokelet and Stabeno 1997)[31], more observations are required to support the existence of this counter current.

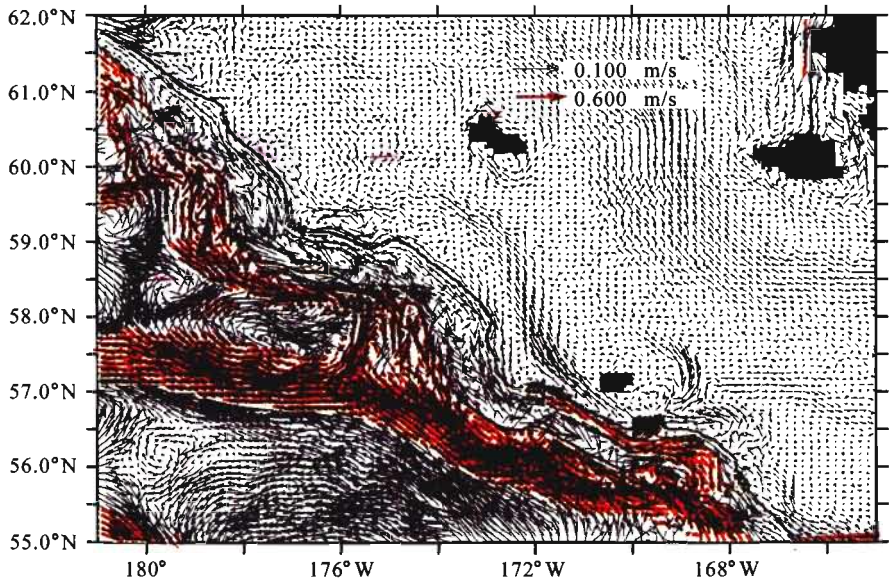

Fig. 8 Model-simulated shelf break counter current. Black arrows indicate current velocity smaller than 10 cm/s and red arrows indicate current velocity greater than 10 cm/s. The February vertically averaged currents in the slope and shallow shelf basically flow northward or northwestward, while the shelf break counter current (5-10 cm/s) flows southeastward almost along the 200-m isobath (the green contours).

3.5 Vertical features in the shelf break-slope area

Nutrient transport from deep basin to the shelf is considered to be one of the main factors for high primary productivity on the shelf break, such as in the Bering Sea Green Belt[32,33]. Overlying the continental slope, the shelf break front separates the shelf water from the deep basin water. Available data show that this front persists throughout the year[34].

The velocity of the Bering Slope Current (Figure 9a) is about 40 cm s^{-1}, flowing northwestward along about 1000-m isobath, which is located at a downwelling (about 10^{-5} m s^{-1}) area (Figure 9b). The shelf break counter current flows southeastward along about 200-m isobath (Figure 8), corresponding to the upwelling area (Figure 9b).

The simulated temperature (Figure 9c) and salinity (Figure 9d) fronts on the shelf break (at depth at 80-120 m) are clearly captured. The 4.5-5.5°C isotherms at 80-120 m tend to be bended beneath. There is a salinity gradient change from 32.4 to 33.0 psu, which corresponds to the upwelling area (Figure 9b). This upwelling band may be one of the mechanisms that can maintain the Green Belt by pumping the nutrient-rich subsurface water upward to the upper layer.

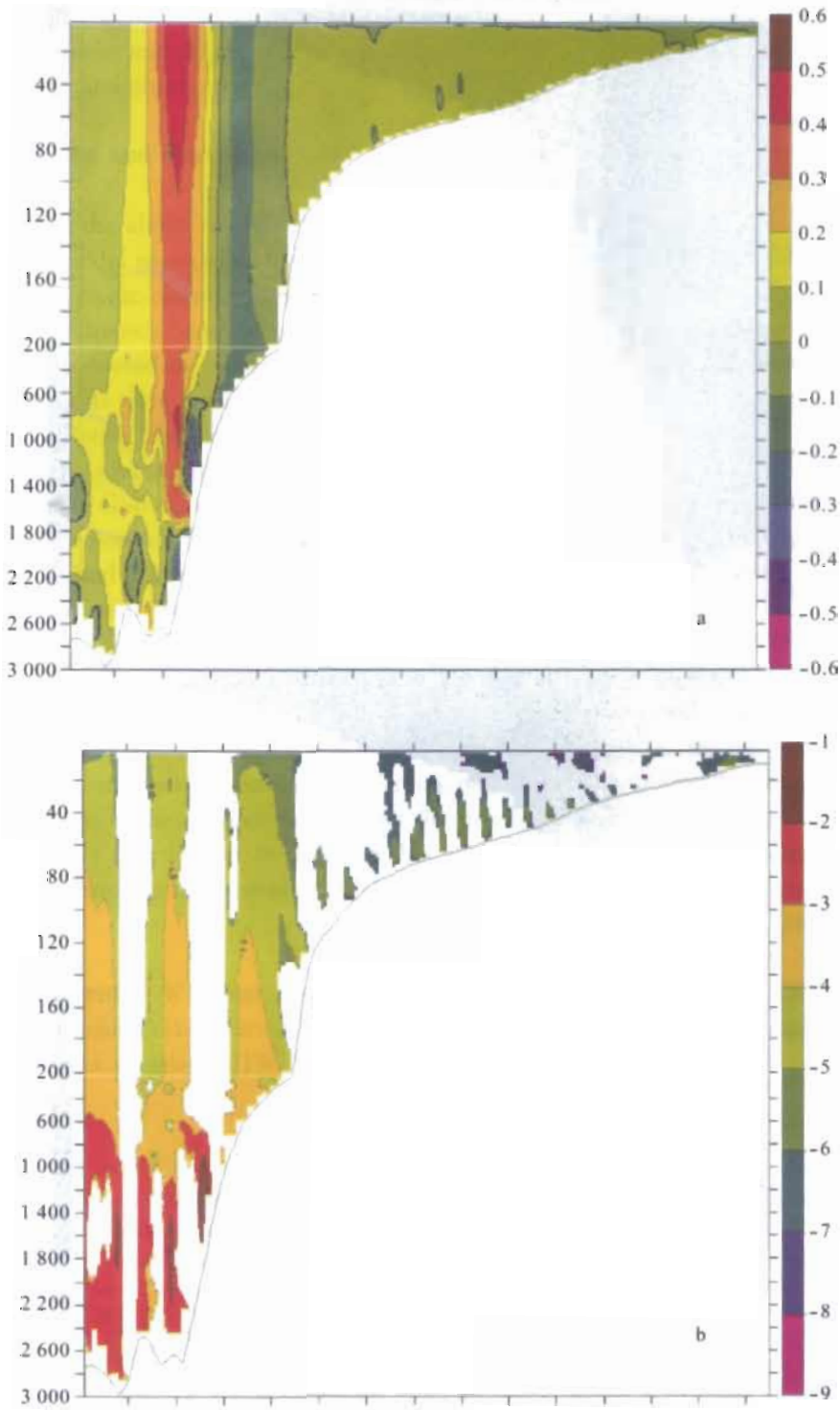
40
80
120
160
200
600
1 000
1 400
1 800
2 200
2 600
3 000
0.6
0.5
0.4
0.3
0.2
0.1
0
-0.1
-0.2
-0.3
-0.4
-0.5
-0.6
a
40
80
120
160
200
600
1 000
1 400
1 800
2 200
2 600
3 000
-1
-2
-3
-4
-5
-6
-7
-8
-9
b

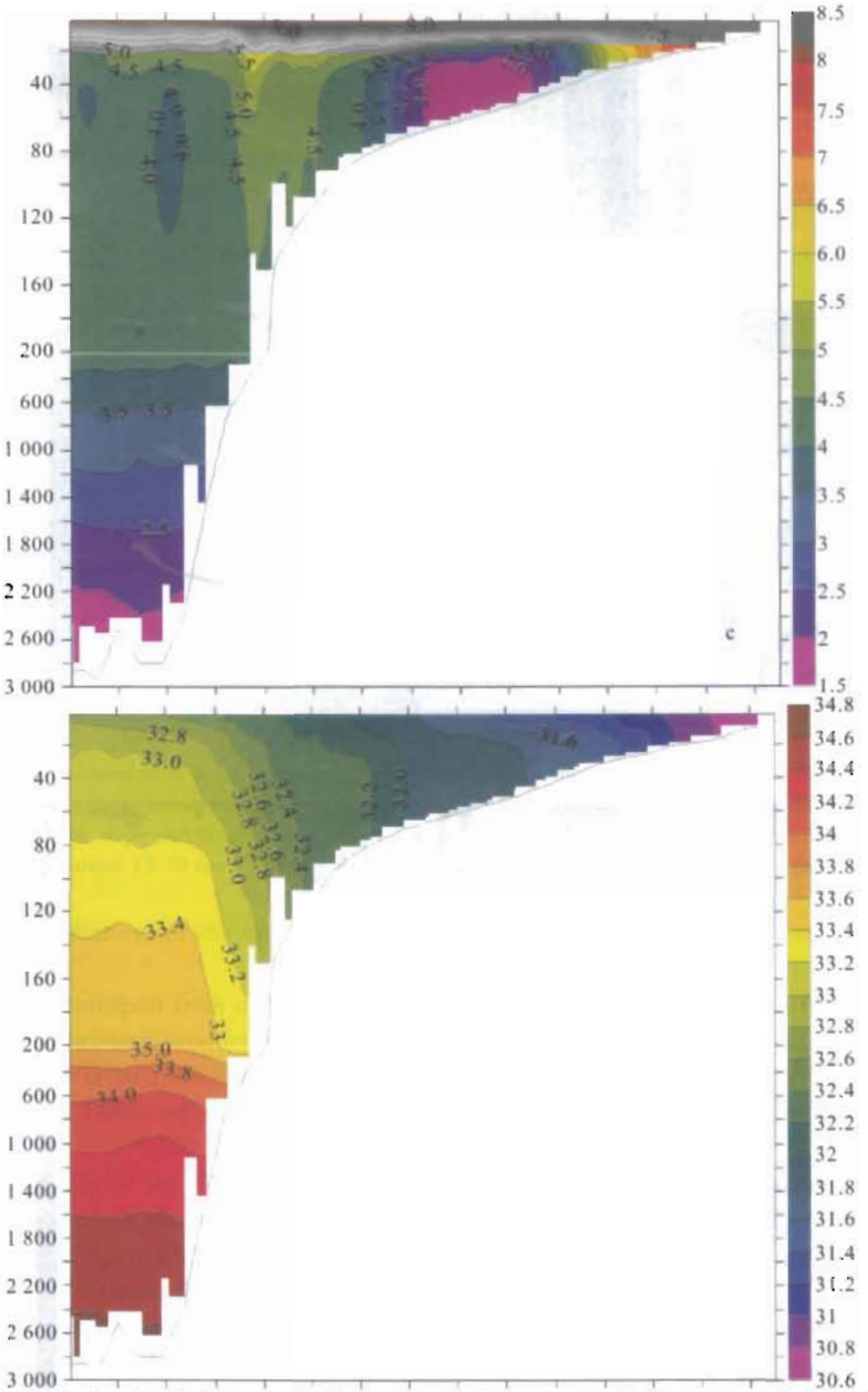

Fig. 9 Model-simulated vertical features in the shelf break-slope areas. (a) Along-shore velocity (m/s) normal to the section, values > 0 indicate the northwestward flow, and < 0 indicate the southeastward flow. (b) Logarithm of vertical velocity log (w). The colored area is upwelling and the blank area is downwelling. (c) Temperature (°C); the isotherms tend to bend beneath in the shelf-break area (80-120 m), and (d) Salinity (psu); there is a salinity front between 33.4 and 34.0 psu in the shelf-break area (80-120 m).

The mechanisms of the upwelling and downwelling as simulated could be very complex. Mesoscale eddies may be one of the causes that can cause convergence and divergence zones near troughs and ridges of a mesoscale eddy[33,35]. This needs detailed research by both modeling and observations.

4 Conclusions and discussion

Based on the above results, the following conclusions can be drawn:

1) The model reproduced the observed circulation pattern. The circulation in the deep basin has a cyclonic circulation with little seasonal changes. The deep basin transports are a result of barotropic, baroclinic, and wind-driven circulation. The overall general circulation pattern is steered by topography and superimposed by multiple large gyres. The major current transports were compared reasonably to observations.

2) The Bering Shelf currents are weak and northward or northwestward with seasonal variations. The winter current is stronger than in summer due to predominant wind forcing. In contrast, the Gulf of Anadyr Current is stronger in summer than in winter due to stronger barotropic transport via the Bering Strait. In the inner shelf, the circulations in Bristal Bay and Norton Sound are cyclonic in summer compared to the anticyclones in winter, comparing reasonably with the previous measurements.

3) A counter current was captured, which flows southeastward along 200 m isobath against the Bering Slope Current, is located at an upwelling area on the shelf break (120-1000 m). However, its existence needs to be proven by systematic observations. The mechanisms of this current may be due to the entrainment of both the Bering shelf water and Bering Slope Current water. Strong wind forcing may be responsible for the counter current. The mechanisms of the counter current and the mechanisms of upwelling and downwelling regions were not investigated in depth in this study. More observational, numerical, and theoretical research is recommended to identify these processes and mechanisms in the near future.

Acknowledgments We thank supports from IARC/JAMSTEC Cooperative Agreement, University of Alaska Costal Marine Institute, and NOAA RUSALCA International Polar Year modeling project awarded to JW. This is GLERL Contribution No. 1502.

References

[1] Wang J, Mooers CNK(1997): Three-dimensional perspectives of the Florida Current: transport, potential vorticity, and related dynamical properties. Dyn. Atmos. & Oceans, 27: 135 - 149.

[2] Stabeno PJ, Schumacher DJ, Ohtani K(1999): The physical oceanorgraphy of the Bering Sea. Dynamics Bering Sea, TR loughlin and K. Ohtani (eds),93 - 127. North Pacific Marine Science Organization (PICES), Published by University by Alaska Sea Grant, Fairbanks, Alaska.

[3] Kinder TH, Schumacher JD (1981a): Circulation over the continental shelf of the southeastern Bering Sea. The eastern Bering Sea shelf: oceanography and resource, vol 1, 53 - 76. DW Hood and JA Calder (eds.), Published by the Office of Marine Pollution Assessment, NOAA and BLM, Distributed by the University of Washington, Seattle, WA 98105.

[4] Overland JE, Spillane MC, Hurlburt HY, Wallcraft AJ(1994): A numerical study of the circulation of

the Bering Sea basin and exchange with the north Pacific Ocean. J. Phys. Oceanogr., 24:736 - 758.
[5] Spaulding M, Isaji T, Mendelsohn D, Turner AC(1987): Numerical simulation of wind-driven flow through the Bering Strait. J. Phys. Oceanogr., 17:1799 - 1816.
[6] Hermann AJ, Stabeno PJ, Haidvogel DB, Musgrave DL(2002): A regional tidal/subtidal circulation model of the southeastern Bering Sea: Development, sensitivity analyses and hindcasting, Deep Sea Res., II (Topical Studies in Oceanography) 49: 5495 - 5967.
[7] Kinder TH, Schumacher JD (1981b), Hydrographic structure over the continental shelf of the southeastern Bering Sea. The eastern Bering Sea shelf: oceanography and resource, vol 1, 31 - 52. DW Hood and JA Calder (eds), Published by the Office of Marine Pollution Assessment, NOAA and BLM. Distributed by the University of Washington, Seattle, WA 98105.
[8] Overland JE, Salo SA, Kantha LH, Clayson CA(1999): Thermal stratification and mixing on the Bering Sea shelf. Dynamics Bering Sea, TR loughlin and K Ohtani (eds), 129 - 146.
[9] Blumberg AF, Mellor GL(1987): A description of a three-dimensional coastal ocean circulation model. in Three-Dimensional Coastal Ocean Models, N. S. Heaps (Ed.), 1 - 16, American Geophysical Union, Washington, DC.
[10] Mellor GL, Blumberg AF(2004): Wave breaking and ocean surface layer thermal response. J. Phys. Oceanogr., 34:693 - 698.
[11] Mellor GL, Yamada T(1982): Development of a turbulence closure model for geophysical fluid problems. Rev. Geophys. Space phys., 20:851 - 875.
[12] Martin PJ(1985): Simulation of the mixed layer at OWS November ans Papa with several models. J. Geophys. Res., 90:903 - 916.
[13] Craig PD, Banner ML(1994): Modeling wave-enhanced turbulence in the ocean surface layer. J. Phys. Oceanogr., 24:2546 - 2559.
[14] Ezer T, Mellor GL(1997): Simulations of the Atlantic Ocean with a free surface sigma coordinate ocean model. J. Geophys. Res., 102(C7): 15,647 - 15,657.
[15] Hu H, Yuan Y, Wan Z(2004): Study on hydrodynamics of Bohai Sea, the Yellow Sea and the East China Sea with wave-current coupled numerical model. Acta Oceanologica Sinica (in Chinese with an English abstract), 4:19 - 32.
[16] Mellor GL, Ezer T, Oey LY(1994): The pressure gradient conundrum of sigma coordinate ocean models. J. Atmos. Oceanic Technol., 11:1126 - 1134.
[17] Mellor GL(2004): User's Guide for a three-dimensional, primitive equation, numerical ocean model, 56pp, Program in Atmospheric and Oceanic Science, Princeton University, Princeton, N. J..
[18] Coachman LK, Aagaard K, Tripp RB(1975): Bering Strait: The Regional Physical Oceanography. University of Washington Press, Seattle, 172.
[19] Coachman LK, Aagaard K(1981): Reevaluation of water transports in the vicinity of Bering Strait. The eastern Bering Sea shelf: oceanography and resource, vol 1, pp 95 - 110. D. W. Hood and J. A. Calder (eds), Published by the Office of Marine Pollution Assessment, NOAA and BLM. Distributed by the University of Washington, Seattle, WA 98105.
[20] Coachman LK, Aagaard K(1988): Transports through Bering Strait: Annual and interannual variability. J. Geophys. Res., 93: 15,535 - 15,539.
[21] Roach AT, Aagaard K, Pease CH, Salo SA, Weingartner T, Pavlov V, Kulakov M(1995): Direct measurements of transport and water properties through Bering Strait. J. Geophys. Res., 100(C9):18, 443 - 18,457.
[22] Woodgate RA, Aagaard K(2005): Revising the Bering Strait freshwater flux into the Arctic Ocean. Geophys. Res. Lett., 32: L02602, doi: 10.1029/2004GL021747.
[23] Cokelet ED, Schall ML, Dougherty DM(1996): ADCP-Referenced geotropic circulation in the Bering Sea basin. J. Phys. Oceanogr., 26: 1113 - 1128.
[24] Onishi H, Ohtani K(1999): On seasonal and year to year variation in flow of the Alaskan Stream in the central north Pacific. J. Oceanog., 55:597 - 608.
[25] Reed RK, Stabeno PJ(1999a): A Recent full-depth survey of Alaskan Stream. J. Oceanogr., 55:77 - 85.

[26] Steele M, Morley R, Ermold W(2001): PHC: A global ocean hydrograph with a high quality Arctic Ocean. J. Climate, 14, 2079 - 14,2087. 24.

[27] Kowalik Z (1999): Bering Sea tides, Dynamics Bering Sea. TR Loughlin and K Ohtani (eds), 93 - 127. North Pacific Marine Science Organization (PICES), Published by University by Alaska Sea Grant, Fairbanks, Alaska.

[28] Reed RK, Stabeno PJ(1999b): The Aleutian North Slope Current. Dynamics Bering Sea, TR loughlin and K Ohtani (eds),177 - 191. North Pacific Marine Science Organization (PICES), Published by University by Alaska Sea Grant, Fairbanks, Alaska.

[29] Panteleev GG, Stabeno P, Luchin VA, Nechaev DA, Ikeda M(2006): Summer transport estimates of the Kamchatka Current derived as a variational inverse of hydrophysical and surface drifter data. Geophys. Res. Lett. 33, L09609, doi:10.1029/2005GL024974.

[30] Overland JE, Stabeno PJ, Salo S (1996): Direct evidence for northward flow on the northwestern Bering Sea shelf. J. Geophys. Res., 101(C4): 8971 - 8976.

[31] Springer AM, Mcroy CP, Flint MV(1996): The Bering Sea Green Belt: shelf-edge processes and ecosystem production. *Fish. Oceanog.*, 5:205 - 223.

[32] Cokelet ED, Stabeno PJ(1997): Mooring observations of the thermal structure, salinity,and currents in the SE Bering Sea basin. J. Geophys. Res., 102(C10):22,947 - 22,964.

[33] Mizobata K, Wang J, Saitoh SI(2006): Eddy-induced cross-slope exchange along the Bering Sea shelf break using a 3D ocean general circulation model and satellite multi-sensor remote sensing. J. Geophys. Res., 111: C10017, doi: 10.1029/2005JC003335.

[34] Kinder TH, Coachman LK(1978): The front overlaying continental slope in the eastern Bering Sea. J. Geophys. Res., 83 (C9):4551 - 4559.

[35] Wang J, Ikeda M(1997): Diagnosing ocean unstable baroclinic waves and menders using quasi-geostrophic equations and Q-vector method. J. Phys. Oceanogr., 27(6): 1158 - 1172.